Synthesis of an Arenide-Masked Scandium Complex Accompanied by Reductively Induced C-H Activation

Alejandra Gómez-Torres, Alejandro Metta-Magaña, and Skye Fortier*

Department of Chemistry and Biochemistry, University of Texas at El Paso, El Paso, Texas 79968

ABSTRACT: Reduction of 3*N*-supported ScCl(^{ket}guan)(NIm^{Dipp}) (**Sc^{Cl}**) with K($C_{10}H_8$) generates the naphthalenide-masked species [(18-c-6)K(μ-η^6:η^4-$C_{10}H_8$)Sc(^{ket}guan)(NIm^{Dipp})] (**Sc^{naph}**) and cyclometallated [K(18-c-6)(Et_2O)][Sc{(DippN)[2-^{i}Pr-6-(*C*Me_2)C_6H_3N]C(NC*H*^{t}Bu_2)}(NIm^{Dipp})(THF)] (**Sc^{C-H}**·Et_2O), the latter formed from a rare instance of oxidative addition of a low valent scandium center across an unactivated C(*sp*^{3})-H bond. Moreover, **Sc^{C-H}** displays solid-to-solution phase dependent tautomerism within the moiety of the scandium metallacyle. Finally, a safe and convenient method is described for the dehydration of $ScCl_3\cdot 6H_2O$.

In our laboratory, we have shown that reduction of 3*N*-supported Ti(^{ket}guan)(NIm^{Dipp})$(OTf)_2$ (^{ket}guan = $[(^tBu_2CN)C(NDipp)_2]^-$; Im^{Dipp}N = [1,3-bis(Dipp)imidazolin-2-iminato]$^-$; Dipp = 2,6-^{i}PrC_6H_3) gives the intramolecularly arene-masked Ti(^{ket}guan)(η^6-Im^{Dipp}N) (**A**).[1] Compound **A** is a titanium(II) synthon and potent reductant that is thermally unstable in solution at room temperature.[1-2] Upon standing, **A** performs intramolecular C-H activation to form the intermediate hydride species, (H)Ti(Im^{Dipp}N)[(DippN)(2-^{i}PrC_6H_3-6-(η^1-CH_2CHCH_3)N)C(NC^tBu_2)] (**B**) that rapidly undergoes β-hydride abstraction to yield cyclometallated Ti(Im^{Dipp}N){(DippN)[2-^{i}PrC_6H_3-6-(η^2-*C*H_2*C*CH_3)N]C(NC^tBu_2)} (**C**) with elimination of H_2.[1] Of note, the initial C-H bond activation event does not occur at the more reactive benzylic methine proton of the isopropyl substituent but rather at the C-H bond of the vicinal -CH_3 group. We have been able to leverage this observed reactivity to promote the catalytic transfer hydrogenation of cyclic olefins as well as the hydrodesulfurization of thiophene.[3-4]

In contrast with its Group 4 and 5 counterparts,[5-6] discrete low-valent complexes (Sc(0), (I), and (II))[7-13] and synthons[14-16] of the more Lewis acidic scandium are significantly more scarce with only a handful of examples reported to date. A successful strategy for accessing low-valent synthons has been the use of arene-masked scandium compounds, which formally possess Sc(III) bound to reduced arenides such as naphthalenide or anthracenide. The ring rearomatization energy provides a driving force for electron transfer that has given way to promising reactivity. For example, Diaconescu's ferrocene-diamide stabilized inverse sandwich $[(NN^{fc})Sc]_2(\mu\text{-}C_{10}H_8)$ (NN^{fc} = 1,1'-$(NSi^tBuMe_2)_2(FeCp_2)$) mediates pyridine reductive coupling[14] and P_4[17] and C-F bond activation,[18] while the half-sandwich analogue $[(THF)_2K(\mu\text{-}C_{10}H_8)Sc(NN^{fc})]$ mediates the reductive coupling of diphenylacetylene affording the respective metallacyclopentadiene.[19] More recently, Okuda et al. reported that the anthracenide-masked $[Li(THF)_3]\{Sc[N(^tBu)(Xyl)]_2(\kappa^2\text{-}C_{14}H_{10})\}$ (Xyl = 3,5-$Me_2C_6H_3$) reduces azobenzene, ultimately yielding the dinuclear complex $\{[(^tBu)(Xyl)N]Sc(\mu\text{-}\eta^2\text{:}\eta^2\text{-}Ph_2N_2)(THF)\}_{2.}$[16] However, it should be noted that reductively induced C-H activation has not been observed with scandium.

We reasoned that by extending our 3*N*-platform to the more electropositive Group 3 metals, in particular neighboring scandium, we may access arene-masked, low-valent synthons with reactivity that exceeds that observed in our titanium complexes.

We have developed a straightforward and safe route for the dehydration of $ScCl_3\cdot 6H_2O$ that avoids the use of hazardous thionyl chloride as a drying agent.[20] Heating refluxing solutions of the hydrate in dioxane with excess Me_3SiCl, followed by drying, and subsequent reflux in THF with excess Me_3SiCl gives $ScCl_3(THF)_3$ (see Supporting Information (SI) for details). This material is used to make $ScCl_2$(NIm^{Dipp})$(THF)_3$[21] that is then reacted with Li$(THF)_2$(^{ket}guan)[22] to give the tetra-coordinate complex ScCl(^{ket}guan)(NIm^{Dipp}) (**Sc^{Cl}**) in 88% yield.

Preliminary attempts to reduce **Sc^{Cl}** using powerful reductants such as KC_8, K°, K/KI, K($C_{14}H_{10}$), and [K(18-c-6)][$C_{10}H_8$][23] under a variety of conditions (e.g., time, temperature, solvent) gave red- or yellow-colored solutions from which no tractable products were isolated. In one instance, reaction of **Sc^{Cl}** with KC_8 over 3 d at -35 °C in toluene yielded a few colorless crystals of [(^{ket}guan)(^{Dipp}ImN)Sc(μ-Cl)$_2$K(DME)]·C_6H_{14} from DME/hexanes (Figure S19). On the other hand, **Sc^{Cl}** reacts with 2 equiv of *in-situ* prepared K($C_{10}H_8$) in THF at -35 °C to rapidly produce a deep red solution. Subsequent addition of 1 equiv of 18-crown-6 followed by crystallization at -35 °C from ethereal solutions yields a mixture of colorless plates and red rhombohedral crystals respectively of cyclometallated [K(18-c-6)(Et_2O)][Sc{(DippN)[2-^{i}Pr-6-(*C*Me_2)C_6H_3N]C(NC*H*^{t}Bu_2)}(NIm^{Dipp})(THF)]·0.5Et_2O (**Sc^{C-}**

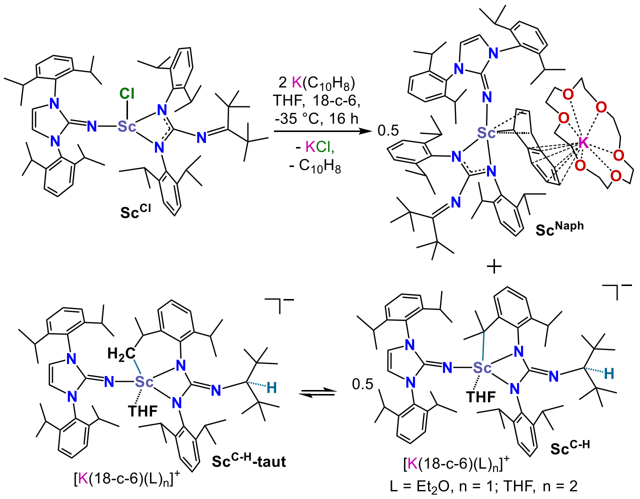

Scheme 1. Synthesis and reduction chemistry of **Sc^{Cl}**.

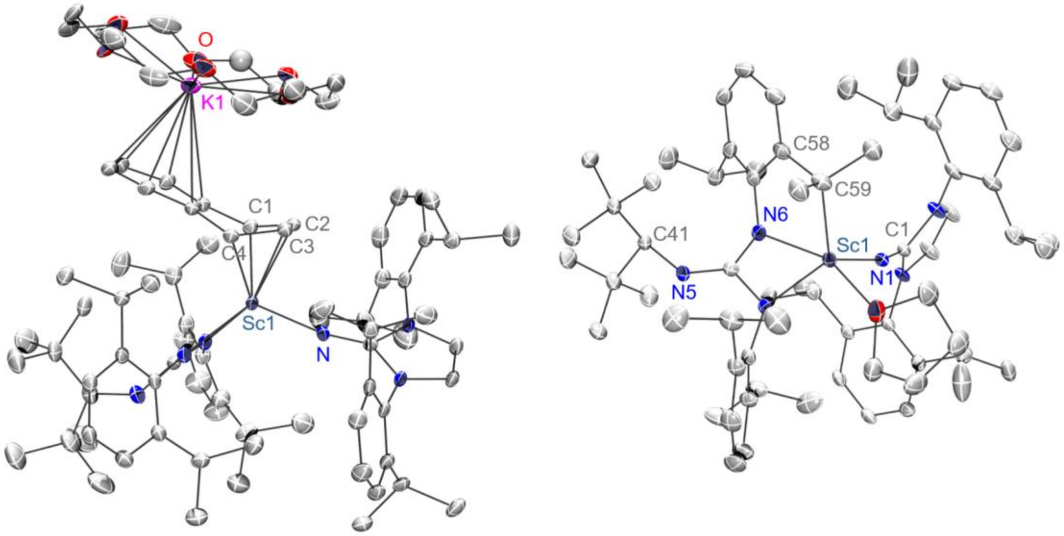

Figure 1. Solid-state molecular structures of **Sc$^{\mathbf{naph}}$** (right) and **Sc$^{\mathbf{C\text{-}H}}$**$\cdot$Et$_2$O (left). Hydrogen atoms, co-crystallized solvents, and the [K(18-c-6)(Et$_2$O)]$^+$ cation of **Sc$^{\mathbf{C\text{-}H}}$**$\cdot$Et$_2$O are omitted for clarity.

$^{\mathbf{H}}$ $\cdot$Et$_2$O) and the reduced naphthalenide species [(18-c-6)K(μ-η^6:η^4-C$_{10}$H$_8$)Sc($^{\text{ket}}$guan)(NIm$^{\text{Dipp}}$)] (**Sc$^{\mathbf{naph}}$**) (Scheme 1).

The products, **Sc$^{\mathbf{C\text{-}H}}$** and **Sc$^{\mathbf{naph}}$**, exhibit nearly identical solubility properties, which makes their separation challenging and frustrates the isolation of pure material in good yields. Therefore, multi-step fractional crystallization is necessary to separate small amounts of **Sc$^{\mathbf{C\text{-}H}}$** (27% isolated yield) from **Sc$^{\mathbf{naph}}$** (36% isolated yield), which is possible due to the slightly higher solubility of **Sc$^{\mathbf{naph}}$** in ethereal or aromatic solvents. The isolation of high purity **Sc$^{\mathbf{naph}}$** is impeded by co-crystallization with **Sc$^{\mathbf{C\text{-}H}}$** and the sensitivity of the molecule (*vide infra*).

Sc$^{\mathbf{naph}}$ crystallizes in the monoclinic space group $P2_1/c$ containing a contact ion pair where the [Sc($^{\text{ket}}$guan)(NIm$^{\text{Dipp}}$)]$^-$ and [K(18-crown-6)]$^+$ fragments are bridged by an η^4:η^6-bound naphthalene unit (Figure 1). The naphthalene exhibits clear structural distortions from planarity with the scandium-coordinated carbon atoms (C1-C4) bending approximately 32° from the ring plane, which has been similarly observed in {(THF)$_3$K(μ-η^4:η^4-C$_{10}$H$_8$)Sc[N(^{t}Bu)(Xyl)]$_2$}.[15] This bending is consistent with reduction of the naphthalene to its dianionic form (C$_{10}$H$_8$)$^{2-}$; however, meaningful bond metric analysis on **Sc$^{\mathbf{naph}}$** is precluded by severe disorder of co-crystallized solvent molecules with the lattice that consequently affects data resolution.

The solid-state molecular structure of **Sc$^{\mathbf{naph}}$** is maintained in solution at room temperature as indicated by the appearance of four characteristic resonances in the ^{1}H NMR spectrum in C$_6$D$_6$ at 5.74, 6.08, 6.99, and 7.22 ppm that appear in a 2:2:2:2 ratio assignable to the protons of the (C$_{10}$H$_8$)$^{2-}$ fragment. These resonances are shifted downfield from the corresponding signals found in {(THF)$_3$K(μ-η^4:η^4-C$_{10}$H$_8$)Sc[N(^{t}Bu)(Xyl)]$_2$} (3.40, 4.13, 5.78, and 6.18 ppm), though comparisons to [(THF)$_2$K(*μ*-C$_{10}$H$_8$)Sc(NN$^{\text{fc}}$)] cannot be made as the high sensitivity of the compound prevented spectral characterization by NMR spectroscopy. The UV-vis-NIR spectrum of **Sc$^{\mathbf{naph}}$** (Figure S23) exhibits absorption bands at λ = 284 and 480 nm, the latter responsible for the dark red color that is comparable to that seen in the reduced arene complexes of scandium {(THF)$_3$K(μ-η^4:η^4-C$_{10}$H$_8$)Sc[N(^{t}Bu)(Xyl)]$_2$} ($\lambda_{\max}$ = 536) and {(THF)$_4$K(μ-η^6:κ^2-C$_{14}$H$_{10}$)Sc[N(^{t}Bu)(Xyl)]$_2$} ($\lambda_{\max}$ = 462).[15]

Complex **Sc$^{\mathbf{C\text{-}H}}$**$\cdot$Et$_2$O crystallizes in the monoclinic space group $P2_1/c$ featuring two crystallographically independent cation/anion pairs in the unit cell with one of the molecules displayed in Figure 1. The solid-state structure displays notable features with the most salient being the presence of a Sc-C bond with the methine carbon of an isopropyl substituent of the ketimine-guanidinate ligand, reminiscent of **C**. It forms a five-member metallacycle that gives the scandium a distorted square-based pyramidal geometry. The Sc-C bond lengths (e.g., Sc1-C59 = 2.315(3) Å) fall within the known range for structurally characterized scandium metallacycles (2.248(3) Å – 2.321(2) Å).[24-32] Furthermore, the Sc-C bond is accompanied by significant bond metric distortions within the guanidinate ligand of **Sc$^{\mathbf{C\text{-}H}}$**$\cdot$Et$_2$O when compared to **Sc$^{\mathbf{Cl}}$**$\cdot$0.5C$_7$H$_8$ (Figure 2). Elongations of the C$_{\text{N3}}$-N$_{\text{Dipp}}$ bonds are seen in **Sc$^{\mathbf{C\text{-}H}}$**$\cdot$Et$_2$O (C40-N4 = 1.390(4) Å;

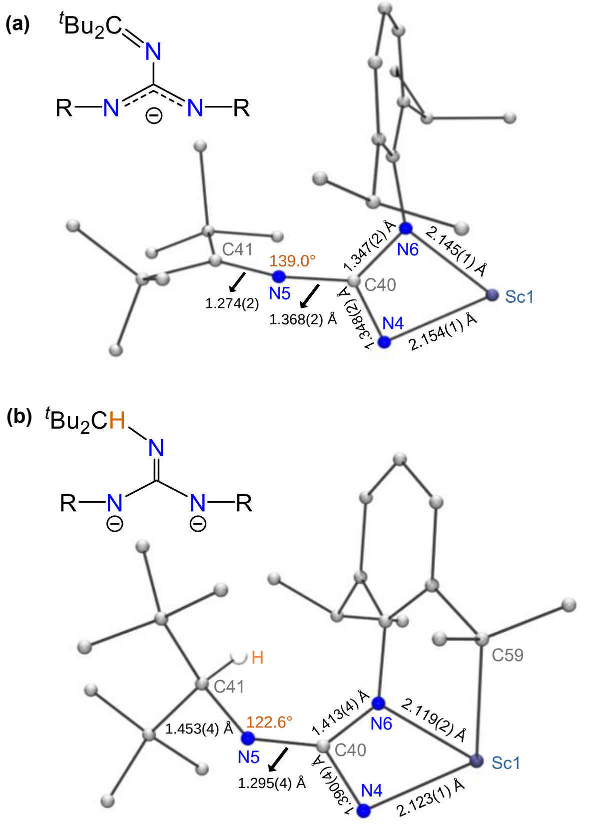

Figure 2. Comparison of selected bond distances in (a) **Sc$^{\mathbf{Cl}}$**$\cdot$0.5C$_7$H$_8$ and (b) **Sc$^{\mathbf{C\text{-}H}}$**$\cdot$Et$_2$O.

C40-N6 = 1.413(4) Å) over those in **Sc^{Cl}**$\cdot 0.5C_7H_8$ (C40-N4 = 1.348(2) Å; C40-N6 = 1.347(2) Å) that is accompanied by shortening of the C40-N5 = 1.295(4) Å bond in **Sc$^{C\text{-}H}$**$\cdot Et_2O$ as compared to C40-N5 = 1.368(2) Å in **Sc^{Cl}**$\cdot 0.5C_7H_8$. Moreover, the N5-C41 = 1.453(4) Å bond distance in **Sc$^{C\text{-}H}$**$\cdot Et_2O$ indicates loss of the N=C double bond character of the ketimine moiety. Contraction of the C40-N5-C41 = 122.6(3)° bond angle of **Sc$^{C\text{-}H}$**$\cdot Et_2O$ is also observed in relation to **Sc^{Cl}**$\cdot 0.5C_7H_8$ (C40-N6-C41 = 139.0(2)°). Altogether, the parameters point to the presence of a dianionic guanidinate ligand where both coordinating nitrogen atoms (N4 and N6) possess formal negative charges. Though unprecedented for scandium, dianionic guanidinate-supported early transition metal complexes are known and exhibit bond metrics similar to those observed in **Sc$^{C\text{-}H}$**$\cdot Et_2O$.[33-40]

The formation of the Sc-C bond and the dianionic guanidinate can be explained via hydride migration from a C-H bond of the isopropyl group to the imine carbon of the ketimine backbone. The presence of the $^tBu_2C(H)$- proton has been confirmed by ^1H NMR spectroscopy, appearing as a singlet at 3.44 ppm in C_6D_6. Based upon our previous observations with **A** and its conversion to **B**, we propose that reduction of **Sc^{Cl}**$\cdot 0.5C_7H_8$ generates an intermediate arene-masked scandium complex of the type $\{Sc(^{ket}guan)(\eta^6\text{-}Im^{Dipp}N)\}^-$ (**Sc-arene**). This species is unstable and rapidly undergoes intramolecular C-H activation to give $\{(H)Sc(Im^{Dipp}N)[(DippN)(2\text{-}^iPrC_6H_3\text{-}6\text{-}(\eta^1\text{-}CH_2CHCH_3)N)C(NC^tBu_2)]\}^-$ (**Sc-H**), signifying passing access to a highly reactive Sc(I) synthon capable of cleaving strong C-H bonds. The proposed **Sc-H** intermediate then undergoes intramolecular hydride transfer, which is surprising as scandium-hydrides are well known to undergo σ-bond metathesis.[41-46] Along these lines, this is a departure from the σ-bond metathesis that occurs in the formation of **C**. This reveals an interesting divergence between the chemistries of scandium and titanium in our system. While intramolecular C-H activation has been previously documented in a number of scandium complexes,[25-31] reductively induced C-H bond activation with scandium is unprecedented. Though, C-H bond cleavage has been reported in the vapor condensation synthesis of $Sc(\eta^6\text{-}^tBu_3C_6H_3)[\eta^7\text{-}(CH_2CMe_2)^tBu_2C_6H_3]$.[7]

In solution, **Sc^{naph}** is unstable, and slowly converts to **Sc$^{C\text{-}H}$** accompanied by the loss of naphthalene over the course of several days at room temperature (Figure S15). However, it is unlikely that **Sc^{naph}** is the direct precursor to **Sc$^{C\text{-}H}$** in the reduction of **Sc^{Cl}** based upon the slow rate at which the conversion happens. Instead, it is likely that elimination of naphthalene from **Sc^{naph}** produces either **Sc-arene** or a "naked," coordinatively unsaturated Sc(I) species that subsequently undergoes oxidative addition across the C(sp^3)-H bond.

Curiously, the solution phase spectra of crystalline **Sc$^{C\text{-}H}$**$\cdot Et_2O$ does not match the structural arrangement observed in the solid-state. This compound has been thoroughly characterized by 1D and 2D NMR correlation spectroscopy (^1H, $^{13}C\{^1H\}$, ^{13}C DEPT, COSY, TOCSY). Namely, in solution, the metalation is observed at the methyl carbon of the isopropyl group to give the tautomer $[K(18\text{-}c\text{-}6)(Et_2O)][Sc\{(DippN)[2\text{-}^iPr\text{-}6\text{-}(CH_3CH\mathit{CH_2})C_6H_3N]C(NC\mathit{H}^tBu_2)\}(NIm^{Dipp})(THF)]$ (**Sc$^{C\text{-}H}$-taut**). In C_6D_6, the Sc-CH_2 protons appear together as a poorly resolved multiplet (Figure S5) due to signal overlap, but the TOCSY spectrum shows clear coupling of the protons within the $CH_3CH\mathit{CH_2}$-Sc moiety (Figure S8). In THF-d_8, the Sc-CH_2 signals are resolved into two separate peaks (Figure S9) that shows the protons to be diastereotopic with an ABX splitting pattern with peaks at -0.60 (H_A) and -0.50 (H_B) ppm along with the proton of the methine carbon appearing as a broad signal at 3.79 ppm (H_X).

Dissolving crystals of **Sc$^{C\text{-}H}$**$\cdot Et_2O$ followed by recrystallization does not change its molecular structure in the solid-state. Crystals can be grown from THF, affording **Sc$^{C\text{-}H}$**$\cdot$THF (Figure S17), giving the same methine-activated solid-state structure. To test whether the tautomerization occurs as a function of temperature, variable temperature NMR spectra show no change within the metalated isopropyl group of **Sc$^{C\text{-}H}$-taut** down to -40°C (Figure S10), which is below the -35°C temperature used in the crystallization of **Sc$^{C\text{-}H}$**$\cdot Et_2O$. We are not aware of other examples of phase dependent tautomerization in inorganic complexes, though it has been reported in small organic molecules,[47-50] and we tentatively ascribe the phenomenon as a result of crystal packing effects.

In summary, we have described the reduction chemistry of the scandium(III) chloride complex **Sc^{Cl}** using $K(C_8H_{10})$ to afford a mixture of two products, **Sc^{naph}** and **Sc$^{C\text{-}H}$**. X-ray crystallographic analysis of **Sc^{naph}** reveals a naphthalene masked scandium complex where the structural features are in accordance with a $(C_8H_{10})^{2-}$ ligand coordinated to a Sc(III) center. The solid-state molecular structure of **Sc$^{C\text{-}H}$**$\cdot Et_2O$ shows a number of changes and is marked by formal hydride transfer from an isopropyl substituent to the ketimine backbone of the guanidinate, generating a dianionic guanidinate ligand. This transformation likely occurs through oxidative addition of a putative Sc(I) center across an intramolecular C-H bond to give a reactive Sc-H species, the first example of reductively induced C-H activation with a Group 3 metal in a homogeneous solution. Moreover, phase dependent tautomerization is observed in the metalated bond of **Sc$^{C\text{-}H}$**$\cdot Et_2O$. These results show key divergences in the reduction chemistry of scandium versus titanium within the same 3*N*-platform. Future work will focus on exploring the reactivity of **Sc^{naph}** as a Sc(I) synthon.

ASSOCIATED CONTENT

Supporting Information.

Experimental procedures and spectral data for **Sc^{Cl}**, **Sc^{naph}**, **Sc$^{C\text{-}H}$**$\cdot Et_2O$, **Sc$^{C\text{-}H}$**$\cdot$THF, and X-ray structure of $[(^{ket}guan)(^{Dipp}ImN)Sc(\mu\text{-}Cl)_2K(DME)]\cdot C_6H_{14}$.

Accession Codes.

CCDC 2176216, 2176217, 2194112, 2194113, 2194416 contain the supplementary crystallographic data for this paper. These data can be obtained free of charge via www.ccdc.cam.ac.uk/data_request/cif, or by emailing data_request@ccdc.cam.ac.uk, or by contacting The Cambridge Crystallographic Data Centre, 12 Union Road, Cambridge CB2 1EZ, UK; fax: +44 1223 336033.

AUTHOR INFORMATION

Corresponding Author

*E-mail: asfortier@utep.edu

ORCID

Skye Fortier: 0000-0002-0502-5229
Alejandra Gómez-Torres: 0000-0002-2663-0807
Alejandro Metta-Magaña: 0000-0001-9993-8485

Notes

The authors declare no competing financial interest.

ACKNOWLEDGMENT

We are grateful to the Welch Foundation (AH-1922-20200401) for financial support of this work. S.F. is an Alfred P. Sloan research fellow and is thankful for their support. We also wish to acknowledge the NSF-MRI program for providing funding for the purchase of an X-ray diffractometer (CHE-1827875).

REFERENCES

1. Aguilar-Calderón, J. R.; Metta-Magaña, A. J.; Noll, B.; Fortier, S., C(sp^3)−H Oxidative Addition and Transfer Hydrogenation Chemistry of a Titanium(II) Synthon: Mimicry of Late-Metal Type Reactivity. *Angew. Chem. Int. Ed.* **2016**, *55*, 14101-14105.
2. Aguilar-Calderón, J. R.; Murillo, J.; Gomez-Torres, A.; Saucedo, C.; Jordan, A.; Metta-Magaña, A. J.; Pink, M.; Fortier, S., Redox Character and Small Molecule Reactivity of a Masked Titanium(II) Synthon. *Organometallics* **2020**, *39*, 295-311.
3. Gómez-Torres, A.; Aguilar-Calderón, J. R.; Encerrado-Manriquez, A. M.; Pink, M.; Metta-Magaña, A. J.; Lee, W.-Y.; Fortier, S., Titanium-Mediated Catalytic Hydrogenation of Monocyclic and Polycyclic Arenes. *Eur. J. Chem.* **2020**, *26*, 2803-2807.
4. Gómez-Torres, A.; Aguilar-Calderón, J. R.; Saucedo, C.; Jordan, A.; Metta-Magaña, A.; Pinter, B.; Fortier, S., Reversible oxidative-addition and reductive-elimination of thiophene from a titanium complex and its thermally-induced hydrodesulphurization chemistry. *Chem. Commun.* **2020**, *56*, 1545-1548.
5. Beaumier, E. P.; Pearce, A. J.; See, X. Y.; Tonks, I. A., Modern applications of low-valent early transition metals in synthesis and catalysis. *Nat. Rev. Chem.* **2019**, *3*, 15-34.
6. Fortier, S.; Gomez-Torres, A., Redox chemistry of discrete low-valent titanium complexes and low-valent titanium synthons. *Chem. Commun.* **2021**, *57*, 10292-10316.
7. Cloke, F. G. N.; Khan, K.; Perutz, R. N., *η*-Arene complexes of scandium(0) and scandium(II). *J. Chem. Soc., Chem. Commun.* **1991**, 1372-1373.
8. Arnold, P. L.; Cloke, F. G. N.; Hitchcock, P. B.; Nixon, J. F., The First Example of a Formal Scandium(I) Complex: Synthesis and Molecular Structure of a 22-Electron Scandium Triple Decker Incorporating the Novel 1,3,5-Triphosphabenzene Ring. *J. Am. Chem. Soc.* **1996**, *118*, 7630-7631.
9. L. Arnold, P.; Geoffrey N. Cloke, F.; F. Nixon, J., The first stable scandocene: synthesis and characterisation of bis(*η*-2,4,5-tri-tert-butyl-1,3-diphosphacyclopentadienyl)scandium(II). *Chem. Commun.* **1998**, 797-798.
10. Neculai, A. M.; Neculai, D.; Roesky, H. W.; Magull, J.; Baldus, M.; Andronesi, O.; Jansen, M., Stabilization of a Diamagnetic ScIBr Molecule in a Sandwich-Like Structure. *Organometallics* **2002**, *21*, 2590-2592.
11. Clentsmith, G. K. B.; Cloke, F. G. N.; Green, J. C.; Hanks, J.; Hitchcock, P. B.; Nixon, J. F., Stabilization of Low-Oxidation-State Early Transition-Metal Complexes Bearing 1,2,4-Triphosphacyclopentadienyl Ligands: Structure of [{Sc(P$_3$C$_2{}^t$Bu$_2$)$_2$}$_2$]; ScII or Mixed Oxidation State? *Angew. Chem. Int. Ed.* **2003**, *42*, 1038-1041.
12. Woen, D. H.; Chen, G. P.; Ziller, J. W.; Boyle, T. J.; Furche, F.; Evans, W. J., Solution Synthesis, Structure, and CO$_2$ Reduction Reactivity of a Scandium(II) Complex, {Sc[N(SiMe$_3$)$_2$]$_3$}$^-$. *Angew. Chem. Int. Ed.* **2017**, *56*, 2050-2053.
13. Woen, D. H.; Chen, G. P.; Ziller, J. W.; Boyle, T. J.; Furche, F.; Evans, W. J., End-On Bridging Dinitrogen Complex of Scandium. *J. Am. Chem. Soc.* **2017**, *139*, 14861-14864.
14. Huang, W.; Khan, S. I.; Diaconescu, P. L., Scandium Arene Inverted-Sandwich Complexes Supported by a Ferrocene Diamide Ligand. *J. Am. Chem. Soc.* **2011**, *133*, 10410-10413.
15. Ghana, P.; Hoffmann, A.; Spaniol, T. P.; Okuda, J., Reduced Arene Complexes of Scandium. *Eur. J. Chem.* **2020**, *26*, 10290-10296.
16. Ghana, P.; Spaniol, T. P.; Okuda, J., Scandium Reduced Arene Complex: Protonation and Reaction with Azobenzene. *Chem. Asian J.* **2021**, *16*, 3170-3178.
17. Huang, W.; Diaconescu, P. L., P4activation by group 3 metal arene complexes. *Chem. Commun.* **2012**, *48*, 2216-2218.
18. Huang, W.; Diaconescu, P. L., Aromatic C–F Bond Activation by Rare-Earth-Metal Complexes. *Organometallics* **2017**, *36*, 89-96.
19. Brosmer, J. L.; Huang, W.; Diaconescu, P. L., Reduction of Diphenylacetylene Mediated by Rare-Earth Ferrocene Diamide Complexes. *Organometallics* **2017**, *36*, 4643-4648.
20. Boyle, T. J.; Cramer, R. E.; Fasulo, F. A.; Padilla, N., Solvation coordination compounds of scandium chloride from the dehydration of scandium chloride hexahydrate. *Polyhedron* **2021**, *208*.
21. Panda, T. K.; Trambitas, A. G.; Bannenberg, T.; Hrib, C. G.; Randoll, S.; Jones, P. G.; Tamm, M., Imidazolin-2-iminato Complexes of Rare Earth Metals with Very Short Metal−Nitrogen Bonds: Experimental and Theoretical Studies. *Inorg. Chem.* **2009**, *48*, 5462-5472.
22. Maity, A. K.; Metta-Magaña, A. J.; Fortier, S., Donor Properties of a New Class of Guanidinate Ligands Possessing Ketimine Backbones: A Comparative Study Using Iron. *Inorg. Chem.* **2015**, *54*, 10030-10041.
23. Castillo, M.; Metta-Magana, A. J.; Fortier, S., Isolation of gravimetrically quantifiable alkali metal arenides using 18-crown-6. *New. J. Chem.* **2016**, *40*, 1923-1926.
24. Hajela, S.; Schaefer, W. P.; Bercaw, J. E., Structure of a permethylcyclopentadienyl-[mu]-tetramethylcyclopentadienylmethylene scandium dimer. *Acta Crystallog. C* **1992**, *48*, 1771-1773.
25. Hayes, P. G.; Piers, W. E.; Lee, L. W. M.; Knight, L. K.; Parvez, M.; Elsegood, M. R. J.; Clegg, W., Dialkylscandium Complexes Supported by β-Diketiminato Ligands: Synthesis, Characterization, and Thermal Stability of a New Family of Organoscandium Complexes. *Organometallics* **2001**, *20*, 2533-2544.
26. Knight, L. K.; Piers, W. E.; Fleurat-Lessard, P.; Parvez, M.; McDonald, R., β-Diketiminato Scandium Chemistry: Synthesis, Characterization, and Thermal Behavior of Primary Amido Alkyl Derivatives. *Organometallics* **2004**, *23*, 2087-2094.
27. Chu, J.; Han, X.; Kefalidis, C. E.; Zhou, J.; Maron, L.; Leng, X.; Chen, Y., Lewis Acid Triggered Reactivity of a Lewis Base Stabilized Scandium-Terminal Imido Complex: C–H Bond Activation, Cycloaddition, and Dehydrofluorination. *J. Am. Chem. Soc.* **2014**, *136*, 10894-10897.
28. Mao, W.; Xiang, L.; Alvarez Lamsfus, C.; Maron, L.; Leng, X.; Chen, Y., Highly Reactive Scandium Phosphinoalkylidene Complex: C–H and H–H Bonds Activation. *J. Am. Chem. Soc.* **2017**, *139*, 1081-1084.
29. Clough, B. A.; Mellino, S.; Clot, E.; Mountford, P., New Scandium Borylimido Chemistry: Synthesis, Bonding, and Reactivity. *J. Am. Chem. Soc.* **2017**, *139*, 11165-11183.
30. Mao, W.; Xiang, L.; Maron, L.; Leng, X.; Chen, Y., Nonchelated Phosphoniomethylidene Complexes of Scandium and Lutetium. *J. Am. Chem. Soc.* **2017**, *139* (49), 17759-17762.
31. Xu, C.; Li, G.; Etienne, M.; Leng, X.; Chen, Y., α-C–C agostic interactions and C–H bond activation in scandium cyclopropyl complexes. *Inorg. Chem. Front.* **2020**, *7*, 4822-4831.
32. Jian, Z.; Rong, W.; Mou, Z.; Pan, Y.; Xie, H.; Cui, D., Intramolecular C–H bond activation induced by a scandium

terminal imido complex. *Chem. Commun.* **2012**, *48*, 7516-7518.

33. Tin, M. K. T.; Yap, G. P. A.; Richeson, D. S., Transition Metal Complexes of Guanidinate Dianions: Reactions between Guanidines and M(NMe_2)$_5$ (M = Ta, Nb). *Inorg. Chem.* **1998**, *37*, 6728-6730.
34. Thorman, J. L.; Guzei, I. A.; Young, V. G.; Woo, L. K., Synthesis, Structure, and Reactivity of Zirconium and Hafnium Imido Metalloporphyrins. *Inorg. Chem.* **1999**, *38*, 3814-3824.
35. Thirupathi, N.; Yap, G. P. A.; Richeson, D. S., Mono- and Dianionic Guanidinate Ligands. Reactivity of [^{i}PrNC(N^{i}Pr)$_2$]Ta(NMe$_2$)$_3$ and [(^{i}PrNH)C(N^{i}Pr)$_2$]TaCl(NMe$_2$)$_3$ with Me_3SiCl and ArNC (Ar = 2,6-$Me_2C_6H_4$). *Organometallics* **2000**, *19*, 2573-2579.
36. Zuckerman, R. L.; Bergman, R. G., Mechanistic Investigation of Cycloreversion/Cycloaddition Reactions between Zirconocene Metallacycle Complexes and Unsaturated Organic Substrates. *Organometallics* **2001**, *20*, 1792-1807.
37. Ong, T.-G.; Yap, G. P. A.; Richeson, D. S., Catalytic C=N bond metathesis of carbodiimides by group 4 and 5 imido complexes supported by guanidinate ligands. *Chem. Commun.* **2003**, 2612-2613.
38. Ong, T.-G.; Yap, G. P. A.; Richeson, D. S., Catalytic Construction and Reconstruction of Guanidines: Ti-Mediated Guanylation of Amines and Transamination of Guanidines. *J. Am. Chem. Soc.* **2003**, *125*, 8100-8101.
39. Yi, W.; Huang, S.; Zhang, J.; Chen, Z.; Zhou, X., Reactivity of Scorpionate-Anchored Yttrium Alkyl Primary Amido Complexes toward Carbodiimides. Insertion Selectivity of Y–NHAr and Y–CH_2Ph Bonds. *Organometallics* **2013**, *32*, 5409-5415.
40. Schweizer, P. D.; Wadepohl, H.; Gade, L. H., Zirconium and Hafnium Hydrazinediido Half-Sandwich Complexes: Synthesis and Reactivity. *Organometallics* **2014**, *33*, 1726-1739.
41. Beh, D. W.; Piers, W. E.; del Rosal, I.; Maron, L.; Gelfand, B. S.; Gendy, C.; Lin, J. B., Scandium alkyl and hydride complexes supported by a pentadentate diborate ligand: reactions with CO_2 and N2O. *Dalton Trans.* **2018**, *47*, 13680-13688.
42. Thompson, M. E.; Baxter, S. M.; Bulls, A. R.; Burger, B. J.; Nolan, M. C.; Santarsiero, B. D.; Schaefer, W. P.; Bercaw, J. E., .sigma.-Bond metathesis for carbon-hydrogen bonds of hydrocarbons and Sc-R (R = H, alkyl, aryl) bonds of permethylscandocene derivatives. Evidence for noninvolvement of the .pi. system in electrophilic activation of aromatic and vinylic C-H bonds. *J. Am. Chem. Soc.* **1987**, *109*, 203-219.
43. Piers, W. E.; Shapiro, P. J.; Bunel, E. E.; Bercaw, J. E., Coping With Extreme Lewis Acidity: Strategies for the Synthesis of Stable, Mononuclear Organometallic Derivatives of Scandium. *Synlett* **1990**, *1990*, 74-84.
44. Sadow, A. D.; Tilley, T. D., Homogeneous Catalysis with Methane. A Strategy for the Hydromethylation of Olefins Based on the Nondegenerate Exchange of Alkyl Groups and σ-Bond Metathesis at Scandium. *J. Am. Chem. Soc.* **2003**, *125*, 7971-7977.
45. Sadow, A. D.; Tilley, T. D., Catalytic Functionalization of Hydrocarbons by σ-Bond-Metathesis Chemistry: Dehydrosilylation of Methane with a Scandium Catalyst. *Angew. Chem. Int. Ed.* **2003**, *42*, 803-805.
46. Sadow, A. D.; Tilley, T. D., Synthesis and Characterization of Scandium Silyl Complexes of the Type Cp$^*_2$ScSiHRR'. σ-Bond Metathesis Reactions and Catalytic Dehydrogenative Silation of Hydrocarbons. *J. Am. Chem. Soc.* **2005**, *127*, 643-656.
47. Sanz, D.; Pérez-Torralba, M.; Alarcón, S. H.; Claramunt, R. M.; Foces-Foces, C.; Elguero, J., Tautomerism in the Solid State and in Solution of a Series of 6-Aminofulvene-1-aldimines. *The J. Org. Chem.* **2002**, *67*, 1462-1471.
48. Kleinpeter, E., NMR Spectroscopic Study of Tautomerism in Solution and in the Solid State. In *Tautomerism*, **2013**; pp 103-143.
49. Enchev, V.; Markova, N.; Marinov, M.; Stoyanov, N.; Rogozherov, M.; Ugrinov, A.; Wawer, I.; Pisklak, M., 2-Methylthio-imidazolins: a rare case of different tautomeric forms in solid state and in solution. *Struct. Chem.* **2017**, *28*, 757-772.
50. Murguly, E.; B. Norsten, T.; Branda, N., Tautomerism of 4-hydroxyterpyridine in the solid, solution and gas phases: an X-ray, FT-IR and NMR study. *J. Chem. Soc., Perkin Trans. 2* **1999**, 2789-2794.